In-Situ Geologic Analyzer for Lunar and Martian Surfaces

Joseph P Martin[1], John R Marshall[2], Larry W Mason[3] Dan Scheld[1]
1. N-Science Corp, 2. SETI Institute, 3. Lockheed Martin

Abstract

The miniature instrument with a triple measurement system, works as a robotic field geologist on remote planetary surfaces such as Mars or the Moon. This Mineral Identification and Composition Analyzer (MICA), employs XRF, XRD, and visual imaging for in-situ nondestructive determination of mineralogy and elemental composition of rock or regolith samples. Its key feature is characterizing geological materials without destroying, damaging, or removing the sample from its in-situ location. MICA addresses two key issues: 1) Mars geology/astrobiology relating to physical and chemical evidence of water and its processes and 2) lunar in-situ resource utilization (ISRU). A 1.5 kg MICA prototype was developed and built under NASA MIDP (Mars Instrument Development Project) and demonstrated with calibration samples and natural rocks on the NASA Ames K-9 test rover robotic arm. MICA serves as a reconnaissance sensor, providing rapid, 10-30 minute analyses for making decisions about further analysis, sample collection, or sample return from a planetary surface.

Introduction

To develop an understanding of the formative history and current condition of a planetary environment, measurement approaches ranging from remote sensing from orbiters through sophisticated in-situ measurements on landers and rovers, have been proposed, developed, and employed [Squyers et al 2007]. In particular, a key piece of the knowledge base for this understanding is a good description of the mineralogical state of the planetary material. Previous and current instrument concepts include close-up and panoramic imagers, X-ray fluorescence (XRF) for element composition, laser ablative spectroscopy for element composition, isotopes, and water detection, gas chromatograph/mass spectrometer for element and molecular analysis, and X-ray diffraction (XRD) to define mineralogy.

The instrument planned on the Mars Science Laboratory (MSL) [Grotzinger et al 2007] that comes closest to developing a good mineralogical description is CHEMIN [Bish et al 2006] that used XRF and XRD of the same sample to obtain crystallographic identification (XRD) and elemental identification (XRF) before a descope eliminated the XRF. This instrument, while providing excellent crystallographic analyses, requires acquisition, crushing, and sieving of rock samples to a fine powder (as well as complex sample manipulation within the device), and further is unable to acquire any visual information about the material that it is analyzing. For rapid surveying of rocks and regolith it is important to be able to collect data without having to go through the very time and energy intensive (and high-risk) process of sample retrieval and preparation required by CHEMIN. The visual context of the sample, lost completely with the CHEMIN approach, is equally important for mineralogical identification.

The Mineral Identification and Composition Analyzer (MICA) is a miniature instrument using XRD and XRF and visible imaging of the same sample location to study rock mineralogy and composition. The objective of the MICA project was to demonstrate with flight configured prototype hardware, the mineralogical analysis capabilities of a compact instrument performing X-ray diffraction and fluorescence plus visual imaging of in-situ, totally unprepared rock and regolith samples. It is implemented with a CCD (charge coupled device) X-ray detector, an active X-ray source, and a microscopic imaging camera. The MICA instrument was developed as part of the NASA Mars Instrument Development Project (MIDP) based on preliminary work demonstrating feasibility of the concept of in-situ XRD/XRF [Marshall et al. 1994, 1996; Koppel et al. 1993]. The scientific objective of a MICA instrument that would be developed for a Mars lander mission as a follow-up to the project [Marshal et al. 2004, 2006] is to provide in-situ assessments of the mineralogical and elemental composition of Martian rocks and surface materials. These determinations would be used for deducing Martian climate history and planet formation processes as well as providing quick assessments of the potential of sample return candidate materials. The instrument was proposed for but not selected for the Mars Science Laboratory (MSL) lander/rover for launch in 2009.

The MICA-MIDP project under JPL subcontract was a 3-year program to design and develop a prototype instrument that could be demonstrated on a NASA ground based Mars rover simulator to show an ability to simultaneously acquire XRD and XRF with a highly miniaturized, low mass, low power concept.

This paper is a description of the basic design, implementation, and test of the MICA brassboard that has a sensor head configuration and function of a flight prototype. The description also includes integration and test on the NASA Ames K-9 Mars Rover located at the NASA Ames Research Center Robotics Test Facility.

MICA Approach and Function

The MICA breadboard, prototype, and the intended follow-up Mars lander MICA are based on a combination of X-ray and visible imaging analyses that determine crystallography, sample color and texture, and elemental composition of the samples examined by the instrument. The X-ray analysis is a combination of X-ray diffraction (XRD) measured by reflection from an opaque sample and X-ray fluorescence (XRF). The color imaging is implemented with an imbedded imaging camera with a close-up lens having augmented depth of field.

The basic approach of MICA is to identify mineralogical composition of rocks and/or loose regolith by compressing the methodology of a field geologist into a small instrument that can obtain its results in-situ. Typically a field geologist approaches rocks and soils using a hand lens to identify color, texture, structural fabric, granularity, and crystallinity as clues to potentially interesting candidates for further analysis. The geologist then collects samples and brings them to the lab, examining them with a petrographic microscope for granularity, inclusions, color, and surface morphology, performing XRF to determine the elements contained in the sample, and finally crushing and grinding the sample into a fine powder to obtain XRD patterns to characterize the particular minerals in the sample.

The XRD patterns typically are compared to standard XRD patterns for pure minerals, where the Joint Committee on Powder Diffraction Standards (JCPDS) catalogs the angular distribution of relative diffraction intensities for known minerals. The relative intensities represent the frequency of occurrence of the various crystal planes at the proper Bragg angles in a random assembly of a large number of sample pieces (powder) within the X-ray beam extent. In the MICA approach, the sample is left intact without crushing and grinding and thus can have less than a large number of randomly oriented pieces within the X-ray beam. The various crystal planes will still diffract X-rays but with relative intensities different from the standard for the crystal, derived from a powdered sample. However, the diffraction angles will still be identical to the standard, simply with different relative intensities, depending on how representative of a random assembly of crystallites the intact sample is; some Bragg angles could even have zero intensity.

The MICA approach, illustrated in Figure 1, departs from traditional powder diffraction in another very significant way in that the X-rays impinge on the sample at a low glancing angle and the diffracted X-rays are detected simultaneously at all scattering angles intercepted by the CCD detector, over a range of scattering planes.

The approach depends on using the visual color, texture, structural fabric, granularity, and crystallinity information about the crystal from the embedded microscopic imager to narrow the range of possible minerals in the sample. It then uses the quantitative elemental analysis derived from XRF to further limit the possibilities. The XRD is then used to look for characteristic Bragg angles for the mineral candidates remaining after visual and XRF analyses. The XRD is thus able to identify some of the crystal plane spacings even though all of them might not have the same relative diffraction intensities as one would see in a powdered sample. This process allows identification of the mineralogy in the sample's undisturbed state.

The MIDP-MICA instrument is eminently suited for dual function as both a contact instrument for analyzing in-situ rocks or regolith or for analysis of crushed rock samples delivered from an on-board sample processing system. For in-situ analyses the sensor head is placed against a rock or regolith by the robotic arm and held there during the analysis.

MICA illuminates the sample at a grazing incidence angle (~8°) and detects the X-rays forward scattered from an area ~320 µm x 45 µm of the surface. Conventional XRD that performs grazing incidence from a thick powdered sample usually scans a detector along an arc in a single plane that encompasses the range of Bragg 2-theta angles. MICA, on the other hand uses an X-ray CCD to detect simultaneously both the isotropic XRF and XRD X-rays at all the relevant Bragg 2-theta angles and record the X-rays from a range of crystal orientations as opposed to the arc in a single plane.

This capability of detecting a range of crystal orientations allows for detection of XRD peaks from a sample whose crystallites are larger than the powdered samples and would therefore not necessarily have crystallites oriented at exactly the right direction for the arc along a single plane. Consequently, one sees on the map, illustrated in Figure 1, of XRD hits on the CCD, a distribution of spots forming the locus of diffraction arcs. If the sample were a fine powder the distribution of spots would look like a continuum along the arcs. The net result is that one can identify, not only the

mineralogy of the sample, but also estimate the grain or crystallite size distribution from the intensity and frequency of the spots along the arcs. This capability of showing grain size distribution in the range of 5 to 60 µm is complementary to the imaging from the embedded imager that shows grain size distributions ≥ 25 µm. The grain size distribution is very important in assessing the geologic history of the sample. We note that this type of grain-size information is completely destroyed in a powder diffractometer such as CHEMIN.

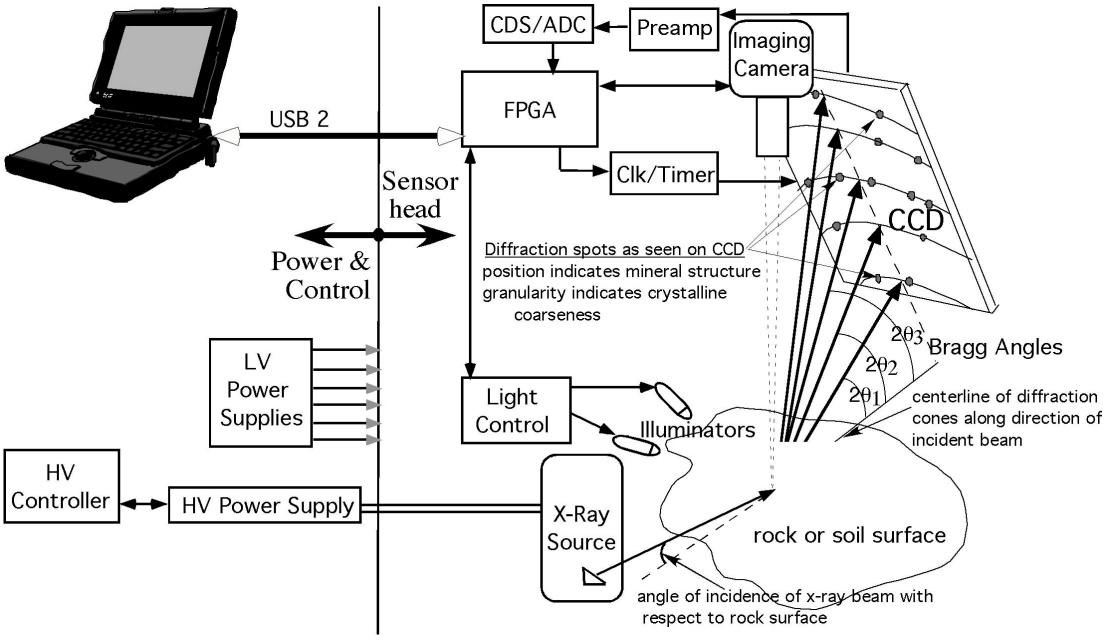

Figure 1. MICA Concept Schematic

MICA Implementation

MICA is packaged as two components, 1) Sensor Head on the end of the rover arm, and 2) Power & Control Assembly on the rover. The prototype included the fully configured sensor head plus laboratory equivalents of the rover mounted components.

In the XRD/XRF and imaging geometry illustrated in Figure 1, the grazing incident X-rays are scattered and detected by the X-ray CCD at 2θ angles from 22° to 62°. The electronic circuit components required for control and operation of the X-ray CCD, the CCD temperature control, light source, the microscopic imager, and a fine position control are all packaged in the Sensor Head. All the software for control, operation and data acquisition and processing is contained in Labview based software in the MICA computer supplemented by a field programmable gate array (FPGA) in the sensor head. The sensor head configuration seen in Figure 2 has a cylindrical lower section containing the X-ray source, X-ray CCD, thermal control elements, illuminator LEDs for imaging, and a mechanism for aperture opening. For thermal control, the outer surface is divided into two thermally decoupled radiators.

The rectangular upper section contains the electronic circuit boards identified in Fig 1 plus the imaging camera. The boards include a preamplifier for X-ray CCD output, an A-D converter/correlated double sampler, a clock/timer, and FPGA plus an auxiliary board for support functions such as thermal and LED control.

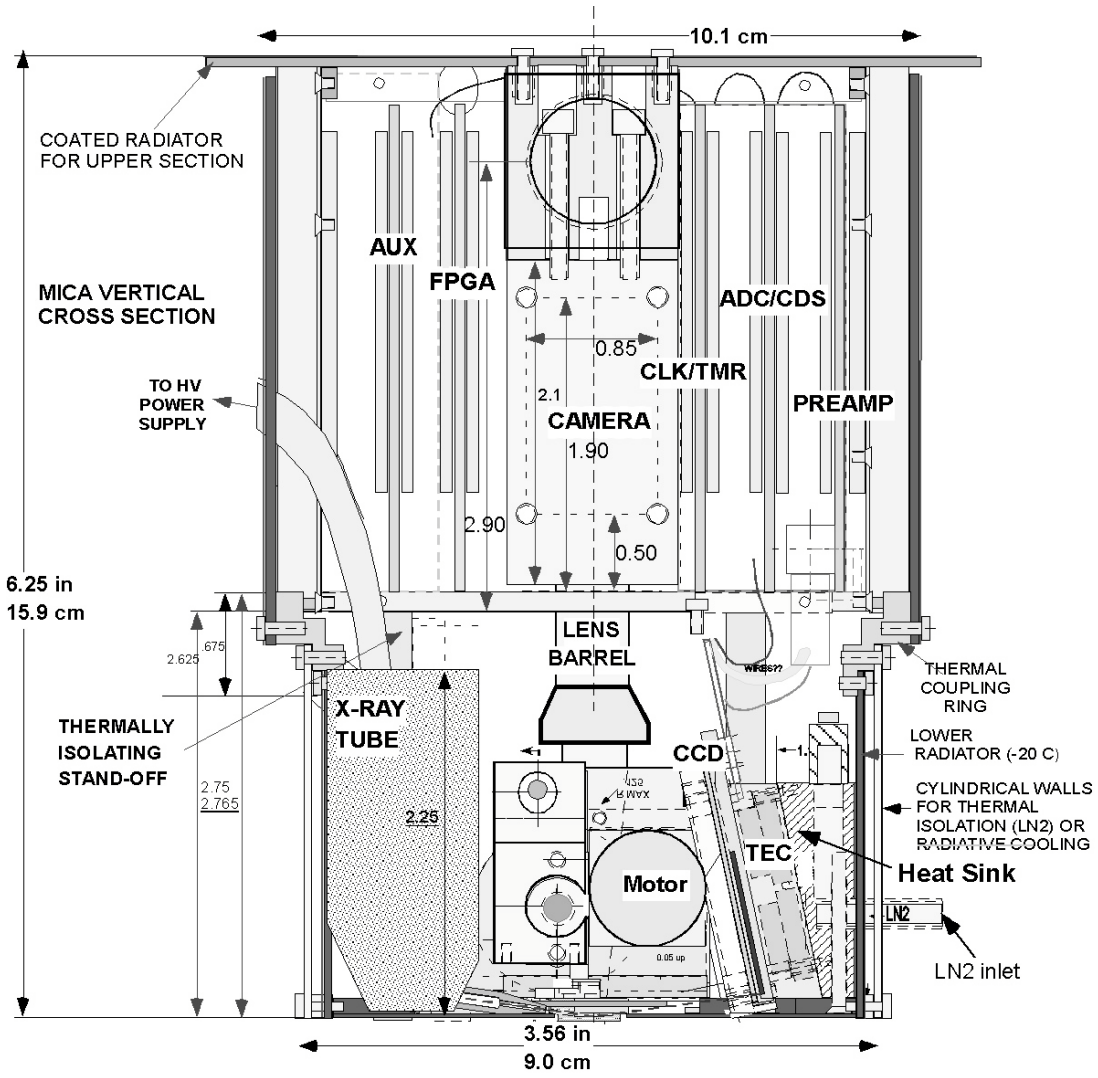

Figure 2. Side View Cutaway MICA Configuration

X-ray subsystem

The X-ray subsystem whose grazing incidence geometry is illustrated in Figure 1 consists of the X-ray tube obtained from Moxtek, an X-ray collimator, the X-ray sensitive CCD focal plane obtained from E2V, a thin light-blocking filter obtained from Luxel, and the associated electronics illustrated by the functional blocks in Figure 1 and the PC boards in Figure 2.

The X-ray source is a miniature Cu reflective anode thermionic tube that operates at 10 to 30 keV and up to 100 µA. It delivers 1.2 E5 photons/s into an angle of 0.3 ° from a 0.4 mm dia. target area. Coupled with the 150 µm dia. collimator and with the anode at a distance of only 25 mm from the sample the photonflux on the sample is sufficient to generate an identifiable rock analysis in 10 to 30 minutes.

The CCD22 is a heritage chip from the European X-ray Camera on XMM-Newton [Turner et al. 2000] that is designed with a deep depletion layer for high X-ray energy (<10keV) sensitivity and at the same time has an open anode structure that allows low energy (<1.5 keV) sensitivity. Its frame transfer structure allows fast transfer (~60

ms) of the entire frame into the store section for subsequent readout while the image section accumulates the next data frame. It has a dual side architecture that reads the two separate sides through split output registers and into separate output FET amplifiers. The CCD22 quantum efficiency (QE) accommodates MICA objectives. The deep depletion augments high energy QE. QE = 0.35 at 8.05 keV Cu k-alpha X-ray for XRD. The open electrode architecture augments low energy QE giving QE = 0.71 for the 1.04 keV Na X-ray for XRF. QE for other geochemically interesting elements is even higher where QE = 0.91for Ca. The CCD has 600 x 600 square 40 µm pixels

The unique advantage of using a CCD for this instrument is that it can accumulate both an XRD diffraction pattern and an XRF energy histogram simultaneously. A CCD pixel that intercepts and interacts with an X-ray photon generates a charge packet proportional to the X-ray energy and the location of the pixel can be translated into a scattering angle for that photon. The data processing circuitry and software identifies both the energy and pixel position. XRD photons are identified by having the full energy (8.05 keV) of the Cu k-alpha from the X-ray tube and are labeled with their pixel position which the analysis software translates to Bragg angles. XRF photons are identified by their energy and are binned accordingly to obtain an energy histogram that translates in to an element spectrum.

Thermal Design

The main drivers of the thermal design are the combination of maintaining the X-ray CCD at an operating temperature below -65°C (208 K) for optimal low dark noise performance while keeping the electronics in the -20° to +40°C operating range in the Mars diurnal temperature excursions.

A MICA system thermal model was developed and used iteratively to design the thermal subsystem [Ladner & Martin 2007]. The CCD thermal subsystem includes the CCD, thermoelectric cooler (TEC), TEC heat sink, passive heat switch, and the subsystem radiator. The TEC holds the CCD focal plane at or below 208 K. Including a TEC and a heat switch between heat sink and radiator significantly extends instrument observation times during Martian diurnal temperature excursions, including atmospheric (~175K to 255K), sky (~130K to 200K), and convection (wind) effects.

The mechanical configuration in Figure 2 shows the structure relevant to thermal control developed in the MICA thermal models. The electronics boards, that dissipate most of the heat, are in the upper rectangular section. The lower cylindrical section contains the X-ray tube and CCD operating at ≤ 208K. The lid and a portion of the upper rectangular surface comprise the *upper* radiator function for the primary thermal dissipation (electronics and X-ray tube), while the lower rectangular section along with the cylindrical surface comprise the *lower* radiator for the CCD subsystem during TEC operation. The two thermally decoupled radiators operate at different temperatures. The rectangular section is covered with silverized Teflon tape to provide good solar rejection and moderately high emissivity; the mostly sun-shaded cylindrical surface has a high emissivity coating. The system thermal model includes *electronics* and *CCD subsystems*. It allows for varying the surface allocation of the fixed mass housing to help tradeoffs between minimum electronics standby power and maximum CCD hold time at 208 K. The preliminary result for MICA is that ~2/3 of the rectangular exterior is needed for the electronics heat rejection.

The CCD subsystem model includes all parasitic and dissipative heat sources, such as heat leaks from electronics, CCD and TEC dissipation during active status, and parasitic heat loads to the focal plane and heat sink. The model incorporates logic that allows the heat switch to provide heat sink cool-down by night and isolation by day if a sufficient temperature difference exists between the radiator and the sink, which must not exceed 258 K for efficient cooler performance. Model parameter variation allows for optimizing the subsystem thermal capacities and resistances to minimize TEC input power and maximize instrument observation time. The results include combinations of heat switch status (open/closed), TEC status (active/inactive), and ambient environmental condition (warm/cold), for various input parameters.

The prototype has a liquid nitrogen path in the TEC heat sink for the system to operate at the proper CCD temperature in the laboratory and a flow of He gas in the interior of the lower section allows less attenuation of low energy X-rays, both unnecessary on Mars or the Moon. The thermal design included the passive thermal switch, which was designed but not built into the prototype.

Imaging Camera

The X-ray analyses are always interpreted in terms of the geologic context as recorded by the microscopic color imaging camera embedded in the center of the sensor head as seen in Figure 2. It images with 2.7 µm resolution a field-of-view (FOV) of 3.8 x 2.9 mm encompassing the X-ray footprint oval of 320µm x 45µm. The optical design shown in Figure 3 provides a front lens-to-sample distance of 57 mm to accommodate the X-ray source and detector geometry.

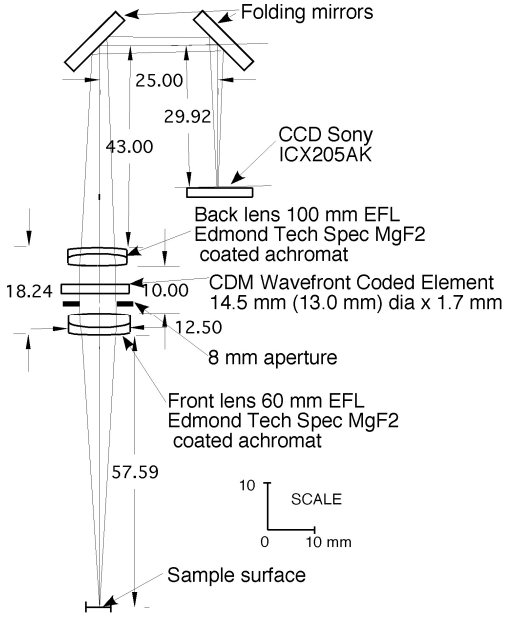

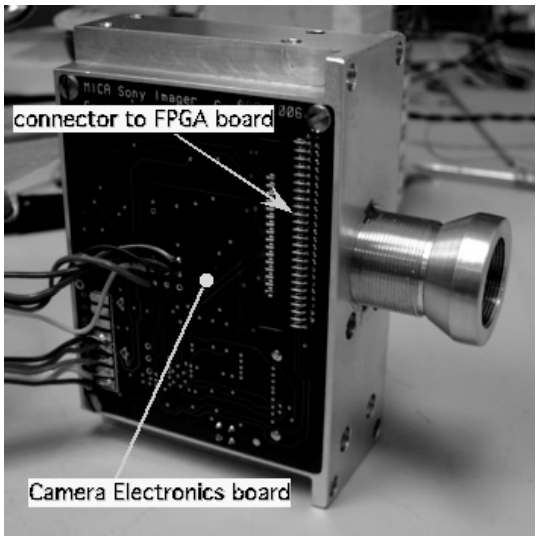

Figure 3. Microscopic Imager Camera

The camera uses a 4-chip set from Sony that includes all the circuitry necessary to run the camera using their ICX205AK CCD, amplifier, A/D converter, and timing generator chips. The imager takes a picture of the sample surface before X-ray operation. LED illuminators in the lower section provide lighting for the picture.

The MICA imager design included depth-of-field (DOF) augmentation demonstrated in the breadboard phase to increase the DOF by a factor of 9.1 to ±750 µm,

but was not included in the final phase due to budget constraints. It uses a wavefront coded optic element seen in Figure 3 from CDM Optics [Cathey et al 2007] and deconvolution software that effectively trades excess modulation transfer function (MTF) at the optimum focus for increased depth of focus with adequate MTF.

Assembled Prototype

The MICA prototype sensor head seen in Figure 4a with the PC boards opened out for testing and in 4b fully assembled shows a mass of 1.44 kg. The power during operation ranges from 5.8-9.6W depending on the TEC cooling needed.

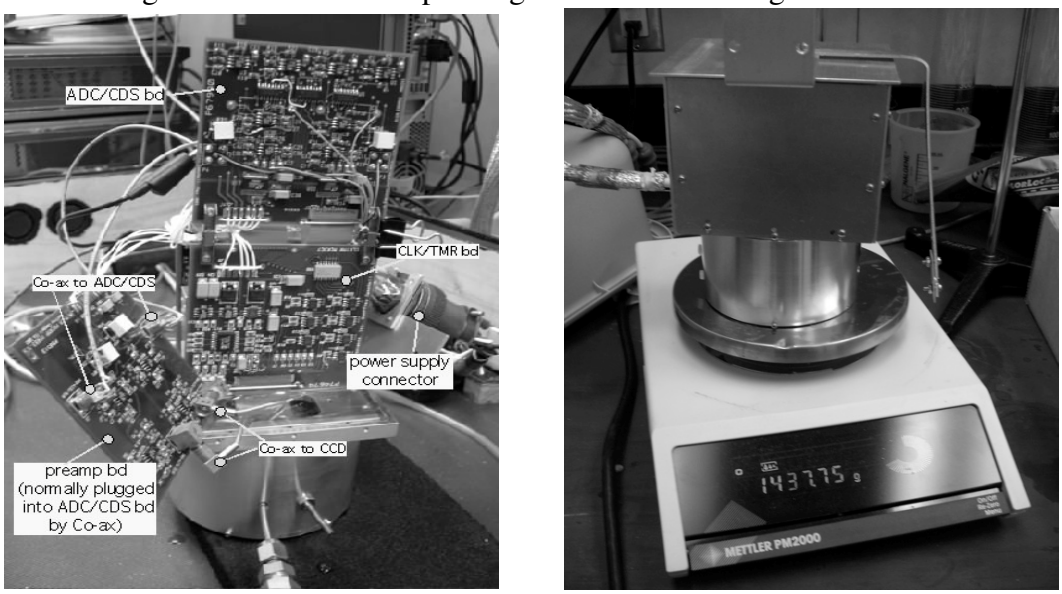

Figure 4. MICA Prototype: (a) PC boards exposed, (b) On scale at 1.44 kg

Data Handling and Analysis

The total data package for a typical 30 min run includes the X-ray CCD data plus one frame of imager data. Uncompressed the X-ray has 600 x 600 pixels x 2 B/pixel x 10 x 10 address bits = 72 MB/frame. A typical 30 min run has 730 frames for 52.6 GB. The lossless compression algorithm developed for MICA resulted in 10 MB for the quartz rock tested in the Rover tests, 8.8 MB for a pipestone sample, and 63 MB for a Mars simulant for 30 min runs. The compression is more efficient when the XRD pattern is more sharply defined. The Mars simulant result was a good example of how this XRD approach identifies highly amorphous samples by showing a radiation hump across the XRD pattern spanning continuously across diffraction angles.

The data for the imager frame at 1024 x 1360 pixels x 2 B/pixel for an uncompressed 2.79 MB/frame. Typical JPEG picture compression yields a reduction by a factor of 10 for 279 kB. Thus the data load is primarily for the XRD/XRF.

The data processing software developed for MICA included not only the data compression and the angular calibration translation for XRD patterns but also 1) discrimination between XRD and XRF data, 2) elimination of split pixel events in XRF data, and 3) XRF Spectrum fitting to identify individual elements.

MICA XRF data accumulated from two tests of desert rock with a surface patina or “desert varnish” illustrates this approach. Test and processing results are seen in Figure 5 (a) on the desert varnish, (b) the same rock with surface patina ground off.

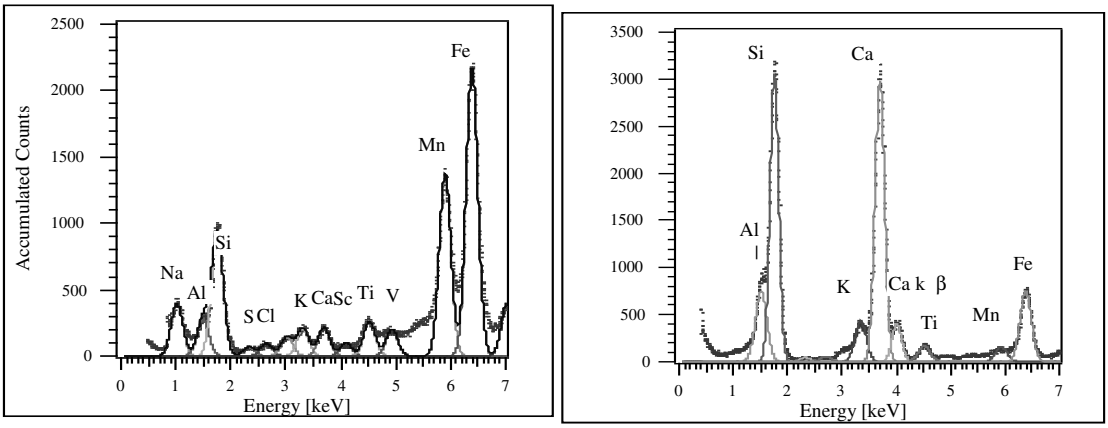

Figure 5. Gaussian fits to desert rock: (a) with desert varnish, (b) fresh cut surface

The approach (1) iteratively calculates attenuation, absorption, scattering, and re-emission of photons in a sample of initially unknown composition, (2), fits the measured data to this model where peaks are expressed as the sum of multiple Gaussian distributions, and (3) integrates the resulting peak areas associated with each element in the energy spectrum. Quantitative elemental abundances are determined by applying known XRF QE values and mass absorption coefficients to the peak areas, and iteratively adjusting the fractions to analytically recreate the measured XRF spectrum.

Testing on NASA K9 Test Rover

MICA on the K9 rover robotic arm at NASA ARC was tested with a Al_2O_3 calibration plate. Figure 6a shows the Labview data screen with the locus of spots representing X-ray hit positions on the CCD; Bragg diffraction arcs are clearly evident. Figure 6b shows the MICA sensor head on the rover arm placed against a natural quartz rock (quartzite). Notice that the data are acquired simply by resting the sensor head on the sample to be interrogated; there is no sample acquisition or processing.

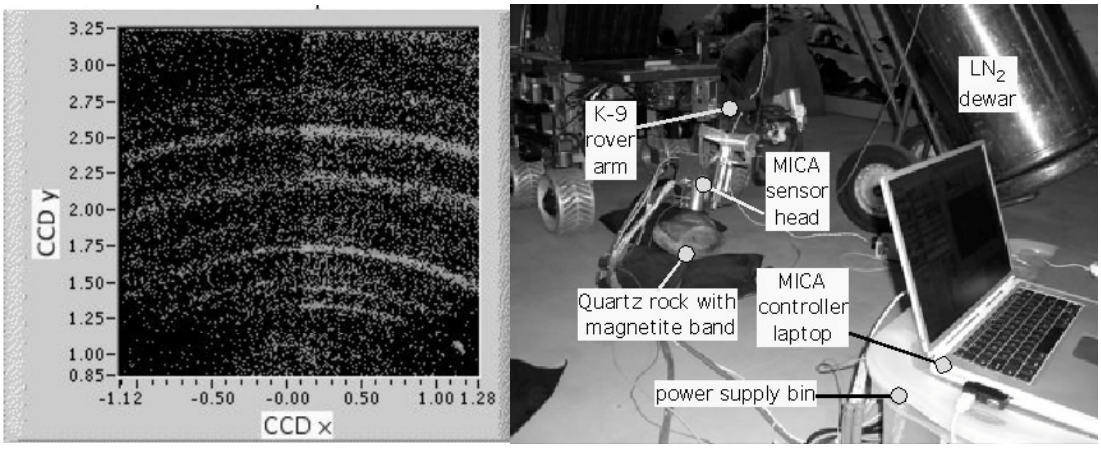

Figure 6. Rover tests: (a) Al_2O_3 calibration; (b) MICA on quartz rock for test

Rover test data in Figure 7a of an XRD data screen, with a sample of undisturbed quartz rock below the sensor head, show the spotty XRD arc segments characteristic of large granular size in a natural rock. This gives information on grain size within the sample, while simultaneously deriving definitive identification of the quartzite, as evident from a comparison with the JCPDS quartz data signature as seen in Figure 7b.

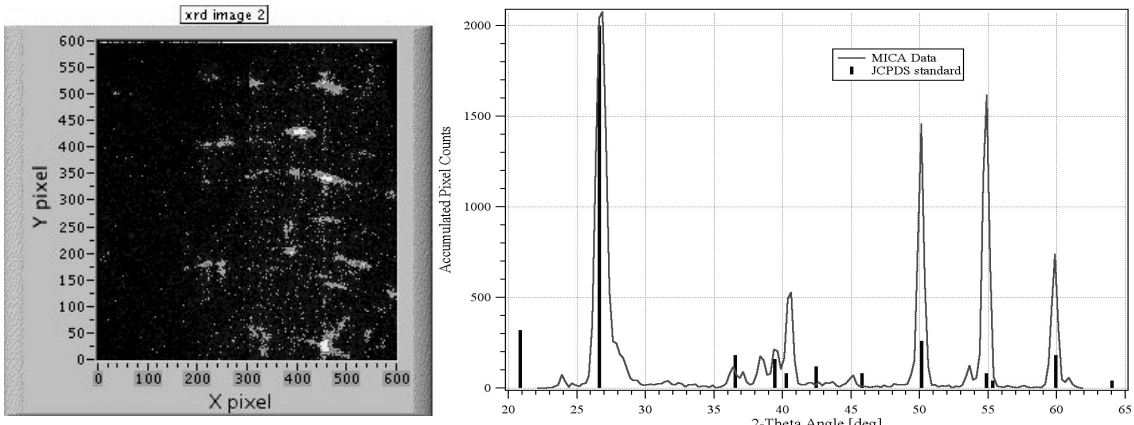

Figure 7. XRD data (a) screen for quartz (b) JCPDS match-up of quartz rock XRD

Summary

A powerful reconnaissance tool for planetary lander/rover operations is demonstrated to simulate a field geologist with capabilities similar to those of his home laboratory. Using XRD, XRF microscopic imaging, and grain-size analysis, the ultra-compact MICA sensor head can be carried on the end of a rover arm to nondestructively assess the mineralogical and elemental state of any material that it can touch. It was proof tested on the NASA K9 rover. It was designed specifically for Mars but is adaptable to any planetary surface.

References

Bish, D., Vaniman, D., Chipera S., Blake, D., Collins, S. (2006) "CHEMIN: A Miniaturized Simultaneous XRD/XRF Instrument" <http://chemin.lanl.gov/> (1/1/08)

Cathey, W.T., Dowski, Edward, Mercure, R.C. (2007) "Wavefront Coded Optics" <http://www.cdm-optics.com/> (12 Dec 2007)

Grotzinger, J., Crisp, J., Vasavada, A., Cook, R., Klein, J., (2007) "Mars Science Laboratory" <http://mars.jpl.nasa.gov/msl/> (28 Dec 2007)

Koppel, L., Franco, E., Kerner, J., Fonda, M., Schwartz, D., Marshall, J. R. (1993) "Integrated XRF/XRD instrument for Mars exobiology and geology experiments" NASA Workshop on Adv Tech for Planetary Instrs, Fairfax, Virginia, April 1993.

Ladner, D., Martin, J. (2007). "Thermal Model for a Mars Instrument with Thermo-Electric Cooled Focal Plane: CCD Subsystem with Heat Switch" Paper C1-M-07 for International Cryogenic Materials Conference at Chattanooga, TN July 2007.

Marshall, J.R., Clark, B.C., & Squyres, S.W. (1994). "An XRF/XRD analyzer for in-situ exploration of the Martian surface." JPL Surveyor Workshop, May 1994.

Marshall, J.R., Bratton, C., Keaten, R., Seward, C., & Koppel, L, (1996) "In situ mineral identification for Mars: Results from a miniature X-ray diffractometer deployed on the Marsokhod rover" Proc. 27th LPSC, 815, 1996.

Marshall, J.R., Martin, J.P., Mason, L.W., & Williamson, D.L. (2004). "In situ analytical strategy for Mars combining X-ray and optical techniques." Proc. 35th Lunar and Planetary Sciences Conference. March 2004, CD-R.

Marshall, J.R., Martin, J.P., Mason, L.W., Williamson, D.L. (2006) "Mineral Identification and Composition Analyzer (MICA) for Mars Instrument Development Project (MIDP) Final Report #EICR-9/06-MICA" Contract # 1248561 submitted to NASA/JPL Sept 30, 2006

Turner, M. J., Abbey, A., (plus 60 others) (2000) "European Photon Imaging Camera on XMM-Newton The MOS Cameras" Astronomy & Astrophysics, Oct 4, 2000

Squyres, S., Arvidson, R., Callas, J. Banerdt, B., Blaney, D. (2007) “The Mars Exploration Program” <http://marsrover.nasa.gov/home/index.html>(26 Dec 07)